Electronic and magnetic properties of Co_{n}Mo_{m} nanoclusters from density functional calculations (n+m=x and 2 ≤x≤6 atoms)

Simon Liebing, Claudia Martin, Kai Trepte, and Jens Kortus

Phys. Rev. B **91**, 155421 — Published 20 April 2015

DOI: 10.1103/PhysRevB.91.155421

Electronic and magnetic properties of Co_nMo_m nanoclusters with $n+m=x$ and $2 \leq x \leq 6$ atoms from DFT calculations

Simon Liebing,* Claudia Martin,* Kai Trepte,* and Jens Kortus*

(Dated: February 18, 2015)

We present the results of our density functional theory study of Co_nMo_m nanoclusters with n+m = x and 2≤x≤6 atoms on the all-electron level using the generalized gradient approximation. The discussion of properties of the pure cobalt and molybdenum cluster is followed by an analysis of the respective mixed clusters of each cluster size x. We found that the magnetic moment of a given cluster is mainly determined by the Co content and increases with increasing n. The magnetic anisotropy on the other hand becomes smaller for larger magnetic moments. We observe an increase in binding energy, electron affinity, and average bond length with increasing cluster size as well as a decrease in ionization potential, chemical potential, molecular hardness and the HOMO-LUMO gap.

Keywords: cobalt-molybdenum ferromagnetic nanoclusters, magnetic properties of nanostructures, Electronic structure of nanoscale materials, modeling and simulation, alloys

I. INTRODUCTION

Transition metal clusters are of interest in various areas of research and application, for example in molecular electronics, long-time magnetic data storage or in the wide field of catalysis[1]. Cobalt clusters have very interesting magnetic properties. There are reports of a very large magnetic anisotropy for the Co-dimer[2–4] making them interesting for possible applications in future storage devices for example in combination with hexagonal carbon rings[5]. It has also been shown that Mo_2X_2 (X = Fe,Co,Ni) clusters are able to act as a spin-filter[6]. Garcia-Fuente et al.[7] computed free-standing $Mo_{4-x}Fe_x$ clusters and came to the conclusion that they are good candidates for molecular electronic devices. These clusters are also widely used as catalysts. In this field, Co-Mo clusters are known to have a strong catalytic effect, for example on the formation of carbon nanotubes[8] or for hydrosulfuration[9,10] (using Co-Mo-S clusters). All these works show that it is necessary to understand the complex interaction of structural and electronic degrees of freedom as well as the influence of different chemical compositions of mixed clusters on the properties of the respective transition metal cluster. These properties govern the possible applicability of the clusters. There are also a few studies on mixed cobalt clusters, for example in combination with manganese[11] and copper[12].

Here we present a density functional theory (DFT) study of the Co_nMo_m nanoclusters with n+m = x and 2≤x≤6 atoms on the all-electron level using the generalized gradient approximation (GGA).

For the pure element clusters there are various studies available concerning the electronic and structural properties, for example for cobalt[3,4,13–20] and for molybdenum (see Ref. [21–23] and references therein) of theoretical and/or experimental nature. The results of these studies will be compared to our results for the pure cobalt and molybdenum clusters. This will be followed by an analysis of the respective mixed clusters of each cluster size x. Finally, we will discuss general trends in structural details as well as in the magnetic and electronic properties.

II. COMPUTATIONAL DETAILS

The starting point is the construction of the metal clusters. On the one hand, the forces in metals are relatively isotropic and therefore we expect most stuctures to be close to finite sphere packings of different sizes[24–27]. This leads to quite compact clusters. As a result, configurations that are far from a spherical structure can be missed. On the other hand, we know that non sphere-like structures can be relevant in atoms[12,20] and cores[28]. Therefore, we have to include at least linear and planar structures. For each investigated structure there exist several stoichiometric compositions between the case of pure cobalt over mixed up to pure molybdenum clusters. Also, the variations in the positions of the atoms towards each other have to be considered.

Smaller clusters up to x = 3 we systematically tested different spin configurations. In case of the larger clusters we started relaxations from $S = 2$ and from $S = 0$. The relaxation algorithm allows for optimization of geometry and magnetic moment at the same time. In the discussion for each geometry and stoichiometry we will focus on the structure lowest in energy that is vibrational stable, too.

All clusters were constructed by the molecular editor Avogadro[29] and preoptimized with its internal force field mechanisms. Then, we perform an unrestricted, all-electron DFT geometry optimization using the NRLMOL program package[30–38]. That includes the freedom to optimize the spin configuration with respect to energy. NRLMOL uses an optimized Gaussian basis set[39], numerically precise variational integration and an analytic solution of Poissons equation to accurately determine the self-consistent potentials, secular matrix, total energies and Hellmann-Feynman-Pulay forces. The exchange correlation is modeled by GGA[40,41] in the form of Perdew-Burke-Enzerhof (PBE)[42]. The relaxation was terminated once forces below 0.05 eV/Å per atom have

been reached. Energetically favored structures are now subject to a stability analysis. First of all the binding energy per atom E_b of the cluster (Co_nMo_m) is considered which is defined as

$$E_b = \frac{\mathrm{n}\ E\,(\mathrm{Co}) + \mathrm{m}\ E\,(\mathrm{Mo}) - E\,(\mathrm{Co_nMo_m})}{\mathrm{m{+}n}}. \quad (1)$$

Here $E_b > 0$ refers to a situation where the total energy of the given cluster is smaller than the sum of its parts, hence the system can save energy by clustering up. For $E_b < 0$ on the other hand one would expect a separation of the cluster into smaller components. Once a cluster proved to be energetically stable we computed the vibrational spectra to check further for dynamical stability: Unstable clusters will show imaginary frequencies.

As some of the stable clusters also showed a magnetic groundstate S, we computed the magnetic anisotropy D. The magnetic anisotropy is mainly due to spin-orbit coupling[43] and can be obtained within DFT via second order perturbation theory[44,45]

$$\Delta_2 \ = \sum_{\sigma\sigma'} \sum_{ij} M_{ij}^{\sigma\sigma'} S_i^{\sigma\sigma'} S_j^{\sigma'\sigma}, \quad (2)$$

where Δ_2 is the second order perturbation energy, σ denotes different spin degrees of freedom and i, j are coordinate labels for x, y, z. Within this framework $S_i^{\sigma\sigma'}$ is defined as

$$S_i^{\sigma\sigma'} \ = \langle \chi^{\sigma} \mid S_i \mid \chi^{\sigma'} \rangle, \quad (3)$$

where χ^{σ} and $\chi^{\sigma'}$ are a set of spinors. These spinors are constructed from an unitary transformation of the S_z eigenstates. The matrix element $M_{ij}^{\sigma\sigma'}$ is given by

$$M_{ij}^{\sigma\sigma'} \ = -\sum_{kl} \frac{\langle \varphi_{l\sigma} \mid \hat{V}_i \mid \varphi_{k\sigma'} \rangle \langle \varphi_{k\sigma'} \mid \hat{V}_j \mid \varphi_{l\sigma} \rangle}{\epsilon_{l\sigma} - \epsilon_{k\sigma'}}, \quad (4)$$

with the occupied and unoccupied states $\varphi_{l\sigma}$ and $\varphi_{k\sigma'}$ and the respective energies $\epsilon_{l\sigma}$ and $\epsilon_{k\sigma'}$. This method can be applied to molecules of arbitrary symmetry and has been used successfully for the prediction of the magnetic anisotropy of various single molecule magnets[46,47]. In the absence of a magnetic field the second order perturbation energy can be rewritten in terms of the anisotropy tensor D_{ij}

$$\Delta_2 \ = \sum_{ij} D_{ij} \langle S_i \rangle \langle S_j \rangle. \quad (5)$$

For a diagonal form of the D_{ij} tensor, the following expression is obtained:

$$D \ = \ D_{zz} - \frac{1}{2}(D_{xx} + D_{yy}). \quad (6)$$

Within this framework, $D < 0$, refers to an easy axis and D$>$ 0 indicates an easy plane system. For an easy axis system the anisotropy barrier U is given by $U \ = \ S^2|D|$. Additionally, we apply the correction proposed by van Wüllen[48].

We also computed ionization potentials IP,

$$IP = \ E(N-1) - E(N), \quad (7)$$

as well as the electron affinities EA

$$EA = E(N) - E(N+1), \quad (8)$$

where N is the total number of electrons in the system. The total energy is sensitive to geometry, charge state and magnetic state. Changes of charge state can also induce changes to the other. In order to get a new total energy for the charged species of the clusters we did a relaxation of structure and spin state. Ionization potential and electron affinity are also closely related to the chemical reactivity which can be described in terms of the chemical potential μ and the molecular hardness η[49,50]. The chemical potential is defined as

$$\mu = -\frac{1}{2}(IP + EA). \quad (9)$$

The molecular hardness is given by

$$\eta = \frac{1}{2}(IP - EA) \quad (10)$$

and accounts for the resistance of the chemical potential to a change in the number of electrons, i.e. it is related to the reactivity of the cluster. Note that the hardness is also related to the HOMO-LUMO gap. A small hardness indicates a small gap and therefore we expect an increase in the reactivity. Here a small gap/molecular hardness leads to a stronger mixing and hence a larger polarizability. A further important quantity is the absolute electronegativity defined as $\chi = -\mu$, where large χ values characterize acids and small χ values characterize bases. All images of clusters are created using Jmol[51].

III. RESULTS

A. General observations

Note that up to m+n = 3 there is always only one conformation for each stoichiometric composition. For larger clusters the number of different variations grows very fast, hence only lowest in energy which are vibrational stable will be discussed in the results.

In all linear clusters except dimers we obtained imaginary vibrational frequencies. This excludes them from further discussion. For the molybdenum we also confirm the trend to form dimer subunits whenever possible[22,23]. In case of investigated planar clusters we find imaginary frequencies in the vibrational spectra of about half of them. Many of them are also energetically less stable than more compact ones. The only planar cluster that is energetically favored over the spherical one is a planar quadrilateral cluster (see Fig.: 2c) with 2 molybdenum and 2 cobalt atoms. Therefore this dimer is the only one that differs significantly from the spherical clusters.

TABLE I: Binding energies E_b in eV, magnetic ground state S, magnetic anisotropy D in K, electron affinity (EA) in eV, ionization potential (IP) in eV, the chemical potential μ in eV, the molecular hardness η in eV, the gap between the highest occupied molecular orbital (HOMO) and the lowest unoccupied molecular orbital (LUMO) in eV as well as the average bond distances in Å for the possible Co_nMo_m clusters

Cluster	S	D [K]	E_b [eV/atom]	EA [eV]	IP [eV]	μ [eV]	η [eV]	Gap [eV]	d_{Co-Co} [Å]	d_{Co-Mo} [Å]	d_{Mo-Mo} [Å]
Co_2	2	-5.6	1.29	0.8	7.3	-4.0	3.2		1.99	-	-
CoMo	$\frac{3}{2}$	13.4	0.83	0.6	6.7	-3.7	3.1	0.58	-	2.48	-
Mo_2	0	-	1.51	0.5	6.7	-3.6	3.1	1.17	-	-	1.98
Co_3	$\frac{5}{2}$	-6.5	1.63	1.4	6.0	-3.7	2.3	0.07	2.21	-	-
Co_2Mo	2	12.5	1.30	1.3	6.2	-3.8	2.4	0.28	2.10	2.48	-
$CoMo_2$	$\frac{1}{2}$	-	1.78	0.8	5.9	-3.4	2.6	0.63	-	2.47	2.07
Mo_3	1	-	1.70	0.7	5.7	-3.3	2.5	0.61	-	-	2.31
Co_4	5	1.0	2.06	1.3	6.1	-3.7	2.3	0.27	2.31	-	-
Co_3Mo	$\frac{5}{2}$	10.7	1.71	1.3	6.1	-3.7	2.4	0.23	2.29	2.39	-
Co_2Mo_2	2	-5.9	2.01	1.5	5.9	-3.7	2.2	0.37	2.18	2.34	2.1
$CoMo_3$	$\frac{3}{2}$	8.5	2.05	1.0	5.6	-3.3	2.3	0.49	-	2.43	2.42
Mo_4	0	-	2.22	0.7	6.7	-3.7	3.0	0.75	-	-	2.52
Co_5	$\frac{11}{2}$	-1.2	2.33	1.6	6.1	-3.9	2.3	0.22	2.34	-	-
Co_4Mo	4	-1.5	2.24	1.1	5.9	-3.5	2.4	0.27	2.29	2.32	-
Co_3Mo_2	$\frac{5}{2}$	-1.6	2.33	1.4	6.2	-3.8	2.4	0.23	2.32	2.38	2.17
Co_2Mo_3	2	6.1	2.32	1.2	5.8	-3.5	2.3	0.48	2.21	2.47	2.35
$CoMo_4$	$\frac{1}{2}$	-	2.38	0.9	5.2	-3.1	2.1	0.28	-	2.46	2.55
Mo_5	0	-	2.48	0.7	5.2	-3.0	2.2	0.58	-	-	2.53
Co_6	7	-0.02	2.70	1.5	6.6	-4.0	2.5	0.45	2.30	-	-
Co_5Mo	$\frac{9}{2}$	-0.6	2.53	1.4	5.9	-3.6	2.2	0.22	2.32	2.37	-
Co_4Mo_2	3	-2.7	2.63	1.5	5.7	-3.6	2.1	0.27	2.33	2.41	2.25
Co_3Mo_3	$\frac{5}{2}$	3.6	2.68	1.6	5.7	-3.6	2.1	0.37	2.32	2.42	2.40
Co_2Mo_4	2	-10.8	2.68	0.5	5.6	-3.1	2.6	0.46	2.26	2.49	2.45
$CoMo_5$	$\frac{1}{2}$	-	2.70	1.1	5.7	-3.4	2.3	0.53	-	2.59	2.50
Mo_6	0	-	2.80	0.1	5.2	-2.7	2.6	0.73	-	-	2.55

B. Dimers

Dimers are the smallest possible class of clusters. Only three different compositions for these nanoclusters are possible and shown in table I. The pure Co dimer, the pure Mo dimer and a mixed CoMo cluster. Within the present study the Mo dimer exhibits a non magnetic ground state ($S=0$) and a binding energy of $E_b=1.5\,\mathrm{eV/atom}$. There has been extensive experimental as well as theoretical research on the Mo dimer. A very nice overview is given by Diez[21], Zhang et al.[22] and more recently by Aguilera-Granja et al.[23] There are reports of calculated binding energies ranging from 1.36 eV to 2.67 eV (see[22] and references therein) depending on the level of approximation used. Older works report even lower binding energies well below 1 eV[52,53]. The experimental value for the binding energies is about 2.2 eV[54–56]. Within the present work the equilibrium distance of the Mo atoms is 1.98 Å, which is in agreement with various theoretical ($d_{Mo-Mo} \sim 1.8$ Å to 2.1 Å[21,22] and references therein) and experimental ($d_{Mo-Mo} \sim 1.94$ Å[54–57]) results. Furthermore, we computed a vibrational frequency $\omega = 533\,\mathrm{cm}^{-1}$, which is in line with other theoretical works ($\omega = 360\,\mathrm{cm}^{-1}$ to $552\,\mathrm{cm}^{-1}$, see Ref. [21] and references therein) and reasonably close to the experimental value of $\omega = 477\,\mathrm{cm}^{-1}$, see Ref. [55,58]. The ionization potential of 6.7 eV is in good agreement with experimental studies (6.4 eV $\leq IP \leq$ 8.0 eV; see Ref. [56] and references therein).

For the Co_2 dimer we calculate a ferromagnetic ground state $S=2$ at an equilibrium distance $d_{Co-Co} = 1.99$ Å which is consistent with previously reported theoretical[3,4,13–20] and experimental[2] values. The $S=2$ ground state indicates a s^1d^8 electronic configuration at each Co atom which is indeed energetically favorable compared to the s^2d^7 electronic configuration[14,15]. Additionally, we report an easy axis magnetic anisotropy. We note that the strength of the anisotropy depends crucially on the bonding distance and therefore also on the energetic ground state. This is in line with the results of Wang et al.[17], who reported low lying quintet states for the Co dimer. Getting the energetic ground state of Co_2 correctly is far from trivial. The predicted ground state and hence electronic structure therefore depends on the exact details (level of approximation for

the exchange-correlation functional, convergence criteria, etc.) of the calculation[3,17,59,60]. As shown in equation (4) the computation of D depends crucially on the electronic structure, hence it is not surprising that we find strong changes in D depending on the details of the calculation. Furthermore we report a binding energy of $E_b = 1.3\,\mathrm{eV/atom}$ which is within the range of previously reported theoretical values (0.87 eV to 5.4 eV, see Ref. [20] and references therein), and close to the experimental value of $E_b \leq 1.4\,\mathrm{eV}$[61,62]. An ionization potential of 7.3 eV is also in good agreement with other experimental ($IP \sim 6.3\,\mathrm{eV}$)[55,62,63] and theoretical ($IP = 6.8\,\mathrm{eV}$ to $7.5\,\mathrm{eV}$)[15,16,20] reports. On the other hand an electron affinity of only 0.8 eV is very small. The computed vibrational frequency of $\omega = 380\,\mathrm{cm}^{-1}$ is comparable to other GGA calculations ($\omega = 340\,\mathrm{cm}^{-1}$ to $420\,\mathrm{cm}^{-1}$)[13,15,16,64], whereas the experimental frequency is given by $290\,\mathrm{cm}^{-1}$ (see Ref. [58]).

The CoMo dimer is dynamically stable with the binding energy ($E_b = 0.8\,\mathrm{eV}$) and shows a $S = \frac{3}{2}$ magnetic ground state with an easy plane magnetic anisotropy of 13.4 K. However, the binding energy is a factor of two smaller compared to the pure Mo_2 and Co_2 resulting in a much larger bonding distance of $d_{\mathrm{Co-Mo}} = 2.48\,\text{Å}$. Additionally, we predict a pronounced Raman feature at $202\,\mathrm{cm}^{-1}$. In general, we see an decrease in the EA as well as in the IP with increasing Mo concentration. This leads to an increase in the chemical potential μ as well as an increase in the molecular hardness η with increasing Co content with Co_2 showing the largest $\mu = -4.0\,\mathrm{eV}$ and $\eta = 3.2\,\mathrm{eV}$.

C. Trimers

There are four different compositions for the trimers all of which are found to be stable as shown in table I and depicted in figure 1. We start from linear and triangular structures. By vibrational stability the linear structures are excluded, such that only the finite sphere packings remain in figure 1.

The Mo_3 cluster shows a S=1 ground state with an increased binding energy $E_b = 1.7\,\mathrm{eV/atom}$ but a shortend average inter-molecular distance of $d = 2.31\,\text{Å}$ compared to the respective dimer. In the result we obtain an asymmetric triangle containing one short bond of 2.14 Å and two longer bonds (2.34 Å and 2.47 Å). This is in accordance to the tendency of dimerization[22,23] due to the half-filled shell of the Mo atoms. But other studies report an more symmetric isosceles structure[21,22,65,66]. The equilateral angle has partly filled degenerated energy levels. This allows for energy lowering by spontaneously symmetry breaking. If the 3 fold symmetry is broken one would expect to find an isosceles structure. Optimizing isosceles structures lead to within numerical errors identical energies as the asymmetric triangle. Even so the obtained structure is not vibrational stable. The oscillation related with imaginary frequency

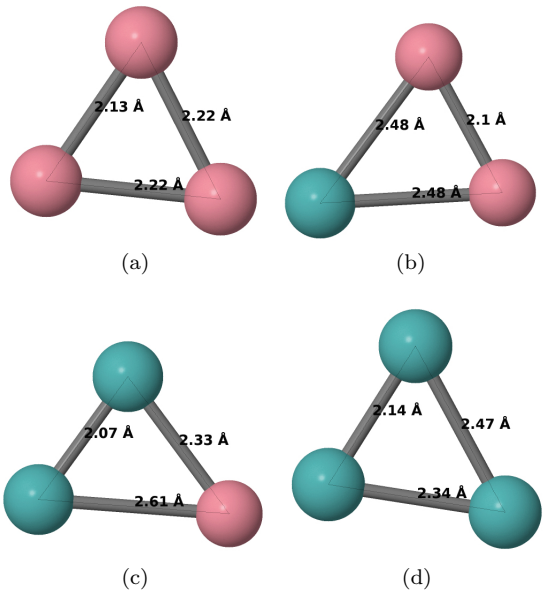

FIG. 1: a): Co_3, b): Co_2Mo, c): $CoMo_2$, d): Mo_3; blue: Mo, red: Co

shows a dimer where the third atom jumps between two metastable configurations close to one or the other side of the dimer. To prevent that the symmetry is further lowered. All the non equilateral triangles contain dimer-like structures, but with respect to energy the position of the third atom is relatively flexible.

This leads consequently to a lower chemical potential ($\mu = -3.3\,\mathrm{eV}$) and molecular hardness ($\eta = 2.5\,\mathrm{eV}$). Note, that the magnetization, binding energy and the inter-molecular distance depends crucially on the symmetry of the Mo triangle. While some studies report a magnetic moment of $0.67\,\mu_B$/atom others predict a magnetic moment of $0\,\mu_B$/atom[21,22,65]. We expect Raman frequencies at $66\,\mathrm{cm}^{-1}$, $220\,\mathrm{cm}^{-1}$ and $406\,\mathrm{cm}^{-1}$ for our lowest energy structure.

For the Co_3 cluster we found a $S = \frac{5}{2}$ ground state with an average distance of $d_{\mathrm{Co-Co}} = 2.21\,\text{Å}$ and a binding energy of 1.7 eV/atom, which is in good agreement with experimental data ($E_b \geq 1.5\,\mathrm{eV}$)[62]. There is an ongoing discussion in literature regarding the energetically favored alignment of three Co atoms. Sebetci[20] and Ma et al[59] predict a linear structure to be the most stable one, whereas several other authors[11,13–16,19] find a triangular structure to be the ground state. According to our calculations the triangular structure is more stable than the linear one and vibrational stable. Also, experimental observations indicate the triangular structure[67]. Bond length in the triangular structure vary from 2.04 Å to 2.24 Å (see Ref. [20] and references therein) and agree well with the computed bond length in the present paper. On the other hand the binding energy ranges from 1.70 eV to 5.34 eV (see Ref. [20] and references therein) where our computed E_b presents an lower bound. The reported ground states for the Co trimer are $S = \frac{7}{2}$ (see

Ref. [14,16,20,59]) and $S=\frac{5}{2}$ (see Ref. [11,13,15,19]), which is consistent with the experimental report of Zee et al.[67] who could not clearly distinguish between $S=\frac{7}{2}$ and $S=\frac{5}{2}$. Ganguly et al[11] observed the same behavior of two degenerated ground states of $S=\frac{5}{2}$ and $S=\frac{7}{2}$. In the present study we also observe a structure with $S=\frac{7}{2}$ which is only 4.5 meV higher in energy than the actual ground state of $S=\frac{5}{2}$. The magnetic ground state depends therefore crucially on the actual geometry. Furthermore, we report an easy axis magnetic anisotropy for the Co trimer resulting in a barrier of 41 K. The ionization potential of 6.0 eV is in good agreement with experimental ($IP=5.97$ eV)[68] and theoretical ($IP=6.6$ eV)[15] results. A larger electron affinity is computed by Perez et al.[12] ($EA=2.6$ eV) compared to the one obtained ($EA=1.4$ eV).

As already observed for the Mo_3 there is again an increase in the electron affinity (0.6 eV) compared to the dimer as well as an decrease in the ionization potential (−1.3 eV). This leads consequently to a lower chemical potential ($\mu=-3.7$ eV) and molecular hardness ($\eta=2.3$ eV). Therefore we expect the Co_3 cluster to be more polarizable and less acidic compared to Co_2.

For the Co_2Mo trimer we obtain a decreased Co-Co distance of 2.1 Å compared to the Co-Co distance in the Co_3 trimer. The Co-Mo distance (2.48 Å) on the other hand remains constant compared to the respective distance in the CoMo dimer (2.48 Å). Magnetically, the Co_2Mo trimer is characterized by a ground state of $S=2$ with an easy plane anisotropy of 12.5 K. Electron affinity (1.3 eV) and ionization potential (6.2 eV) are closely related to those of Co_3 which leads to comparable chemical reactivity in terms of μ and η. Furthermore, we predict pronounced Raman frequencies at 147 cm^{-1}, 186 cm^{-1} and 337 cm^{-1}.

The $CoMo_2$ trimer on the other hand resembles the Mo trimer better with respect to the binding energy, interatomic distances and EA as well as IP (see table I) which is consistent with the amount of Mo within the trimer. Again we observe one short Mo-Mo distance of 2.07 Å which indicates a dimerization of Mo. We report an $S=\frac{1}{2}$ ground state and expect pronounced Raman frequencies at 104 cm^{-1}, 236 cm^{-1} and 388 cm^{-1}.

D. Tetramers

The calculated ground states for the different tetramers are summarized in table I and depicted in figure 2. As we start from finite sphere packing's (tetrahedral structures), linear and square planar structures are considered additionally as initial geometries for the optimization. The linear structures are found to be less stable and/or not vibrationally stable. So the unconstrained optimization provided in all cases except of Co_2Mo_2 to the compact solution.

For the Mo_4 cluster we observe a non magnetic, flattened tetrahedral ground state with a binding energy of 2.2 eV/atom and two different distances of 2.73 Å and 2.10 Å. This underlines the tendency of dimerization in Mo clusters[22,23]. Consequently, ionization potential and electron affinity are nearly identical compared to the dimer.

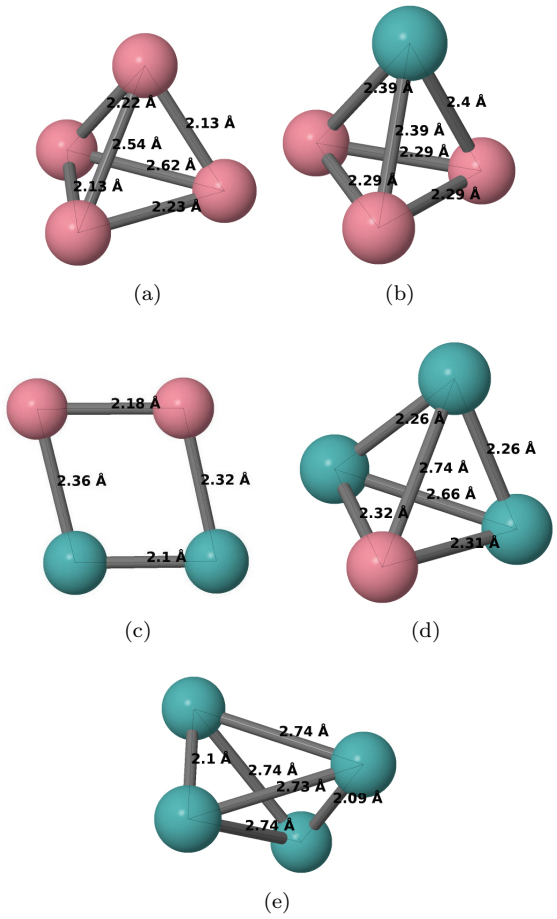

FIG. 2: a): Co_4, b): Co_3Mo, c): Co_2Mo_2, d): $CoMo_3$, e): Mo_4; blue: Mo, red: Co

The structure is also vibrationally stable with pronounced to Raman modes predicted at 145 cm^{-1}, 163 cm^{-1}, 195 cm^{-1}, 435 cm^{-1} and 444 cm^{-1}.

Few studies on the Mo tetramer are available in literature. Min et al[69] report a slightly flattened tetrahedron as the ground state configuration with a binding energy of 3 eV/atom and four equivalent bonds of 2.31 Å and two elongated bonds of 2.63 Å and 2.75 Å length. Diez[21] predict a ground state structure with a binding energy of 2.59 eV/atom and bond lengths of 3.00 Å and 2.23 Å as well as a non-magnetic ground state. Energetically close to that structure they observed a second non magnetic structure with a binding energy of 2.57 eV/atom and bond lengths of 2.62 Å and 2.12 Å. They predict vibrational frequencies of 147 cm^{-1}, 195 cm^{-1}, 213 cm^{-1}, 437 cm^{-1} and 459 cm^{-1}, which is in agreement to the frequencies given in this work. Additionally, they

observed a variety of structures close to the ground state with differing magnetic ground states. Zhang et al.[22] and Aguilera-Granja et al[23] on the other hand predict a rhombic ground state structure with an $S=2$[23] or $S=0$[22] magnetic ground state. However both studies find an isomer close in energy that is nearly identical to the structure reported here and by others[21,69].

The Co_4 cluster on the other hand exhibits a binding energy of 2.1 eV/atom with an equilibrium distance of 2.31 Å. This includes four short bonds and two longer bonds forming again a flattened tetrahedron, which is in line with previous studies[11–13,15,19,70–73]. Other studies[14,20,59] predict a slightly out-of plane rhombus to be the ground state. We get a total magnetic moment of $S=5$ in agreement with previous studies[11–15,20,71,74]. There are also reports of $S=8$ (see Ref. [59]) and $S=9$ (see Ref. [70]). Those studies found the $S=5$ ground state to be slightly higher in energy compared to the respective magnetic ground states reported there. We also found an easy plane magnetic anisotropy of 1.0 K. Furthermore, we report an ionization potential of 6.1 eV, which is in agreement with experimental data ($IP \sim 6.2$ eV)[62,63,68] and reasonably close to other theoretical works ($IP = 5.5$ eV to 5.7 eV)[12,74]. We also found pronounced Raman features at 69 cm^{-1}, 145 cm^{-1}, 211 cm^{-1}, 286 cm^{-1} and 359 cm^{-1}, which is in agreement with previous theoretical work[13,15,20,71].

For the mixed cluster we observe an increase in the total magnetic moment as well as a steady decrease in the binding energy for increasing Co content. For $CoMo_3$ we found a magnetic ground state of $S=\frac{3}{2}$ with an easy plane anisotropy of 8.5 K, a binding energy of 2.1 eV/atom, a slightly larger electron affinity (1.0 eV) and a much smaller ionization potential (5.6 eV) compared to the Mo tetramer. Furthermore we report pronounced Raman features at 73 cm^{-1}, 118 cm^{-1}, 160 cm^{-1}, 182 cm^{-1}, 276 cm^{-1} and 363 cm^{-1}.

For Co_2Mo_2 we find an energetically favored, vibrational stable planar cluster. We predict a $S=2$ magnetic ground state with an easy axis anisotropy of −5.9 K and a binding energy of 2.0 eV/atom.

Co_3Mo has an even higher magnetic ground state of $S=\frac{5}{2}$, an easy plane anisotropy of 10.7 K and a binding energy of 1.7 eV/atom. Electron affinity (1.3 eV) and ionization potential (6.1 eV) are very close to the respective values computed for Co_4. Respectively, we expect a chemical behavior (μ, η) nearly identical to the pure Co tetramer. Pronounced Raman features are expected to be found at 121 cm^{-1}, 194 cm^{-1}, 225 cm^{-1} and 342 cm^{-1}.

E. Pentamers

In the case of pentamers we investigated linear and spherical structures. For spherical ones there are also two different possible structures - square pyramidal (7 possible bonds) and trigonal bipyramidal (9 possible bonds). Six stoichiometric compositions have to be considered. Linear clusters are again found to be unstable. The respective ground state structure and selected properties of those structures are summarized in table I, whereas the ground state geometry can be found in figure 3.

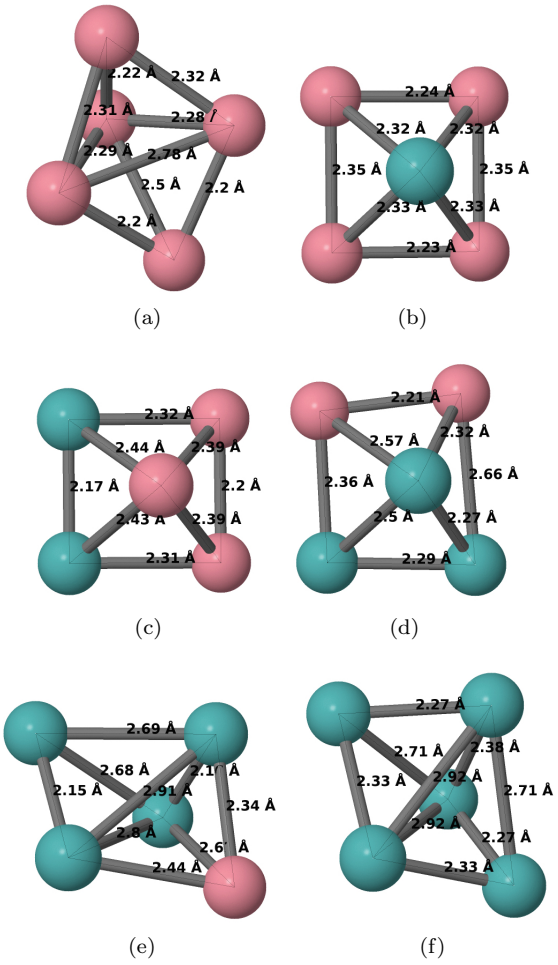

FIG. 3: a): Co_5, b): Co_4Mo, c): Co_3Mo_2, d): Co_2Mo_3, e): $CoMo_4$, f): Mo_5; blue: Mo, red: Co

For the Mo_5 cluster we observe a distorted trigonal bipyramidal ground state structure (which could also be viewed as a distorted square pyramid) with no magnetic moment and a binding energy of 2.5 eV/atom. The average bonding distance is 2.53 Å, with no exceptional short Mo-Mo distances. Hence, the tendency to form dimers seems to be weakened in the pure Mo pentamer which was also observed by others[22]. There is no change in the electron affinity compared to smaller Mo clusters whereas the ionization potential (5.2 eV) is considerably lowered. Consequently, we observe a reduced chemical potential μ and a reduced hardness η compared to smaller clusters. Furthermore, we predict pronounced Raman features at 138 cm^{-1}, 154 cm^{-1}, 169 cm^{-1}, 207 cm^{-1}, 229 cm^{-1}, 290 cm^{-1} and 375 cm^{-1}. Koteski et al[66] reported a similar ground state structure. Zhang et al.[22] report trigonal bipyramidal ground state with $S=0$ with six short

distances of 2.26 Å and three long distances of length 2.77 Å. Very close in energy ($E_b = 0.02$ eV/atom compared to the trigonal bipyramidal structure) they found a pyramid with a rectangular base with bond length of 2*1.94 Å, 2*2.94 Å and 4*2.48 Å. This structure is also non magnetic. Nearly identical results are reported by Min et al[69]. Aguilera-Granja et al.[23] on the other hand predict a 2D fan-like ground state with an $S = 4$ magnetic ground state. This structure was also proposed by Zhang et al.[22] however they reported a binding energy well below the one of the ground state. We checked that structure, in our calculation the binding energy is also lower than of our ground state. Additionally the vibrational spectra contains imaginary frequencies.

For Co_5 we observe the same ground state structure as already mentioned for Mo_5: a distorted trigonal bipyramid or a distorted square pyramid. The structure has a magnetic state of $S = \frac{11}{2}$ with an easy axis anisotropy leading to a barrier of 36 K and a binding energy of 2.3 eV/atom. The average Co - Co distance 2.34 Å with bonds ranging from 2.2 Å to 2.78 Å as depicted in figure 3a. A very similar structure with $S = \frac{13}{2}$ was found only 0.08 eV above the ground state structure. Furthermore we expect pronounced Raman features at 92 cm^{-1}, 116 cm^{-1}, 133 cm^{-1}, 182 cm^{-1}, 204 cm^{-1}, 249 cm^{-1}, 300 cm^{-1} and 334 cm^{-1}. There is no consistent picture in the literature concerning the ground state geometry of Co_5. Sebetci et al[20] report a fan-like 2d structure with $S = \frac{11}{2}$ to be the ground state with energetically close states of a trigonal bipyramidal ($E_b = 0.03$ eV/atom, $S = \frac{13}{2}$) and square pyramidal ($E_b = 0.04$ eV/atom, $S = \frac{11}{2}$) structure. Other studies report a square pyramidal[14,71,74] or trigonal bipyramidal[12,13,19,59,72,73] ground state where the respective other geometry is always very close in energy ($\sim$ 0.15 eV) to the actual ground state. There is also no consensus on the magnetic ground state. We found reports of $S = 4$ (see Ref. [13]), $S = \frac{11}{2}$ (see Ref. [20,59,71,74]), $S = \frac{13}{2}$ (see Ref. [11,12,14,19,72,75]) and $S = \frac{15}{2}$ (see Ref. [73]), where usually a $S = \frac{11}{2}$ or $S = \frac{13}{2}$ magnetic ground state is energetically very close to the actual magnetic ground state. There is also no connection between the ground state geometry and the magnetic ground state in literature.

The experimental ionization potential of 6.2 eV[63,68] is in good agreement with literature ($IP \sim 6$ eV)[72], ($IP = 6.5$ eV)[74] and the one observed in the present study ($IP = 6.1$ eV). Perez et al.[12] on the other hand report a significantly lower ionization potential of 5.1 eV. The ionization potential (6.1 eV) and the electron affinity (1.6 eV) are nearly identical to the Co_3 and Co_4 clusters, hence we would expect a similar chemical reactivity. As already noted for the tetramers, the pentamers of mixed composition show an increase in the total magnetic moment as well as a steady decrease in the binding energy with increasing Co content.

For $CoMo_4$ we obtain a structure that is quite similar to the one of pure Mo_5 with a binding energy of 2.4 eV/atom. It could be described either as a trigonal bipyramid or as a square pyramid with a tilted base (see figure 3e). We see again two very short Mo-Mo distances (~ 2.1 Å) indicating a dimerization of Mo as well as two longer bonds (2.68 Å) and two very long bonds (2.8 Å and 2.9 Å). We found a $S = \frac{1}{2}$ magnetic ground state, a chemical potential and molecular hardness close to Mo_5 and Raman features at 29 cm^{-1}, 93 cm^{-1}, 117 cm^{-1}, 135 cm^{-1}, 171 cm^{-1}, 182 cm^{-1}, 251 cm^{-1}, 358 cm^{-1} and 397 cm^{-1}.

For Co_2Mo_3 the ground state structure resembles a distorted square pyramid with a magnetic moment of S = 2 and an easy plane anisotropy with a binding energy of 2.3 eV/atom. No dimerization of Mo is present, however the average Mo-Mo distance is smaller compared to the tetramers with more Mo content. Additionally, we report Raman frequencies for this structure at 87 cm^{-1}, 104 cm^{-1}, 132 cm^{-1}, 155 cm^{-1}, 183 cm^{-1}, 232 cm^{-1}, 261 cm^{-1}, 296 cm^{-1} and 382 cm^{-1}.

For Co_3Mo_2 the ground state structure has a binding energy of 2.3 eV/atom and resembles a rectangular pyramid as shown in figure 3c with two Mo atoms at neighboring edges and two Co atoms occupying the remaining edges. On the top the residual Co atom is found. With 2.20 Å and 2.17 Å the Co-Co and Mo-Mo distances are quiet short and nearly identical. The Co-Mo distance in the plane is 2.32 Å forming a almost perfect rectangular base of the pyramid. Again we can observe the tendency of dimerization for molybdenum. The ground state has a magnetic moment of $S = \frac{5}{2}$ with an easy axis anisotropy of -1.6 K, an ionization potential (6.2 eV) and electron affinity (1.4 eV) that resembles closely those of Co_5 and Raman features at 59 cm^{-1}, 105 cm^{-1}, 149 cm^{-1}, 204 cm^{-1}, 266 cm^{-1}, 299 cm^{-1} and 386 cm^{-1}.

For the Co_4Mo pentamer we found again a rectangular pyramid with a binding energy of 2.2 eV/atom and a magnetic moment of $S = 4$. It has an easy axis system characterized by an anisotropy of $D = -1.5$ K and a barrier of 32 K. Basis of the pyramid is a rectangle of Co atoms where an atom of Mo lies on top as shown in figure 3b. The ionization potential (5.9 eV) and the electron affinity (1.1 eV) are very close to the respective values of the Co tetramer resulting in a nearly identical chemical reactivity. This indicates that the Mo atom on top is only loosely bound to the structure and does not strongly influence the chemical behavior of the cluster. We also report Raman features at 70 cm^{-1}, 121 cm^{-1}, 133 cm^{-1}, 166 cm^{-1}, 183 cm^{-1}, 247 cm^{-1}, 261 cm^{-1}, 281 cm^{-1} and 349 cm^{-1}.

F. Hexamers

As shown in figure 4a we considered two different possible starting geometries for the hexamer - an octahedral structure (12 possible bonds) and polytetrahedral structure (11 possible bonds). The respective ground state

structure and selected properties of those structures are summarized in table I, whereas the ground state geometry can be found in figure 4b - 4h.

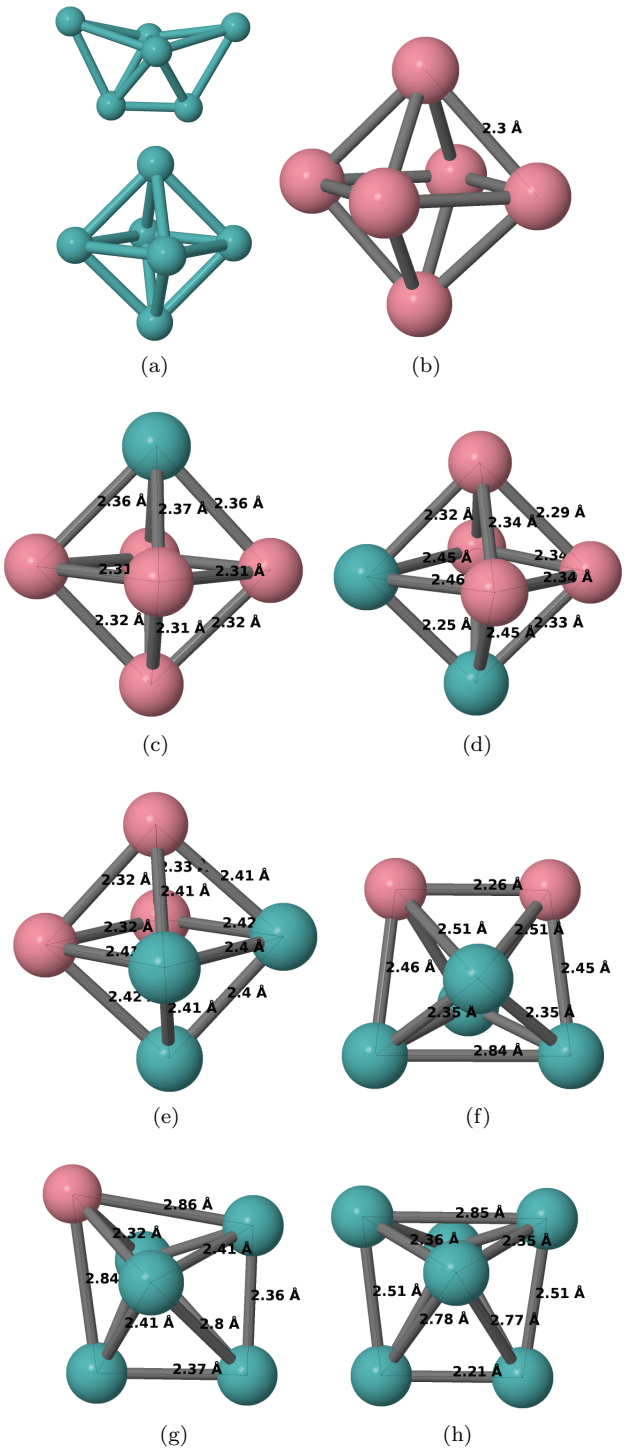

(a) (b) (c) (d) (e) (f) (g) (h)

FIG. 4: a): Co_6, b): Co_5Mo, c): Co_4Mo_2, d): Co_3Mo_3, e): Co_2Mo_4, f): $CoMo_5$, g): Mo_6; all invisible bonds are as long as those directly in front of them. The ground structure of Co_6 is a regular octahedron with an equidistant bond lenght of 2.3 Å. blue: Mo, red: Co

For the Mo_6 cluster we get a distorted polytetrahedral structure as shown in figure 4h which is already close to an octahedral structure with a binding energy of 2.8 eV/atom. The average Mo-Mo distance is 2.55 Å including one very short distance of 2.21 Å at the bottom of the polytetrahedral structure. The structure is non magnetic with a very low electron affinity (0.1 eV) and an ionization potential (5.2 eV) comparable to the one of Mo_5. Accordingly we get a very low chemical potential ($\mu = -2.7$ eV) in comparison to the other structures. Furthermore, we computed Raman frequencies at 62 cm^{-1}, 116 cm^{-1}, 140 cm^{-1}, 199 cm^{-1}, 206 cm^{-1}, 250 cm^{-1}, 341 cm^{-1} and 365 cm^{-1}. Min et al[69] report an octahedral ground state structure with a buckled square base plane and a binding energy of 3.9 eV, whereas other studies[22,23,66] get a non magnetic deformed pentagonal pyramid with a binding energy of 2.92 eV to 3.16 eV.

For the Co hexamer on the other hand we obtain a regular octahedral geometries with a length of 2.30 Å for every bond and a binding energy of 2.7 eV/atom. This regular octahedron has a $S = 7$ magnetic ground state with easy axis anisotropy of -0.02 K. Many previous studies agree on the ground state to be a regular octahedron with $S = 7$, a binding energy of 2.47 eV/atom to 2.98 eV/atom and a Co-Co distance of 2.27 Å to 2.37 Å[12,14,19,70,71,74]. Only Andriotis et al report a significantly larger bond length of 2.67 Å using tight-binding molecular dynamics. Other studies[20,59] reported a distorted octahedron geometry with a $S = 7$ magnetic ground state and an average Co-Co distance of 2.31 Å to 2.39 Å. Moreover we obtained an electron affinity (1.5 eV) close to all previous pure Co_n (n>2) clusters and an ionization potential of 6.6 eV. Especially the IP is in good agreement with previous experimental ($IP \sim 6.2$ eV)[63,68] and theoretical ($IP = 5.07$ eV[12] and $IP = 6.9$ eV[74]) work. We observed Raman features at 193 cm^{-1}, 238 cm^{-1} and 347 cm^{-1}. Sebetci et al. also computed optical frequencies (94 cm^{-1} and 296 cm^{-1}), however they predict a distorted octahedron for the ground state, hence the results may not be comparable.

For the mixed hex-atomic clusters we observe a nice transition from the distorted polytetrahedral structure of pure Mo_6 to a regular octahedron ground state structure as observed for Co_6 with increasing Co-content (see figure 4). This is accompanied by an increase in the total magnetic moment as well as a steady decrease in the binding energy with increasing Co content in agreement with the trends already reported here for smaller mixed clusters.

For $CoMo_5$ we also get a distorted polytetrahedron ground state structure with $S = \frac{1}{2}$ and a binding energy of 2.7 eV/atom. As shown in figure 4g the upper left edge is occupied by the Co atom which has two short bonds (2.32 Å) to the middle Mo atoms and two long bonds (~ 2.85 Å) to the neighboring edges. It could also be viewed as a strongly distorted octehedron with a buckled square base plane where the buckling is due to the Co atom that drags two Mo atoms out of the plane. There

are no very short Mo-Mo distances hence no dimerization occurs. Instead we see six medium size distances (~ 2.38 Å) and two very long bonds of 2.8 Å. Furthermore, we found an ionization potential of 5.7 eV and an electron affinity of 1.1 eV as well as pronounced Raman features at 69 cm^{-1}, 142 cm^{-1}, 200 cm^{-1}, 218 cm^{-1}, 284 cm^{-1} and 351 cm^{-1}.

For Co_2Mo_4 the ground state structure can also be described as a distorted polytetrahedron arrangement with an $S=2$ ground state and an easy axis anisotropy of -10.8 K. Here the upper two edges of the polytetrahedron are occupied by Co atoms forming a short Co-Co bond of length 2.26 Å (see figure 4f). They form two shorter bonds (2.45 Å) to the remaining two edges and four longer, equidistant bonds (2.51 Å) to the center Mo atoms thereby pushing them downwards. This results in four short Mo-Mo bonds (2.35 Å) and one very long Mo-Mo bond (2.84 Å). Again this structure could be also described as a distorted octahedron with a buckled square base plane, where the buckling is due to the Co atoms as already discussed for the $CoMo_5$ hexamer. The ionization potential of 5.6 eV and electron affinity (0.5 eV) are lower compared to the $CoMo_5$ cluster and we report Raman frequencies at 94 cm^{-1}, 115 cm^{-1}, 148 cm^{-1}, 177 cm^{-1}, 194 cm^{-1}, 225 cm^{-1}, 184 cm^{-1} and 356 cm^{-1}.

The Co_3Mo_3 cluster on the other hand resembles clearly a distorted octahedron with a binding energy of 2.7 eV/atom. Again there is no dimerization of the Mo atoms observed, on the contrary all Mo-Mo bonds are equidistant (2.4 Å). Although the other bonds are equidistant, dependent on there bond partners, 2.32 Å for Co-Co bonds and 2.42 Å for Co-Mo bonds. The ionization potential of 5.7 eV is very close to the one of Co_2Mo_4, whereas the electron affinity is considerably larger (1.6 eV). Furthermore, we see Raman features at 131 cm^{-1}, 172 cm^{-1}, 230 cm^{-1}, 293 cm^{-1} and 364 cm^{-1}, a magnetic ground state of $S=\frac{5}{2}$ and an easy plane anisotropy ($D=3.6$ K).

The Co_4Mo_2 ground state structure is also an octahedron with a binding energy of 2.6 eV/atom, a magnetic moment of $S=3$ and an easy axis anisotropy ($D=-2.7$ K). We report a very short Mo-Mo distance (2.25 Å) indicating the already discussed dimerization of Mo due to its half-filled shell. The average Co-Co distance is 2.33 Å with only slight deviations for the different Co-Co distances (2.29 Å to 2.34 Å). On the other hand for the Co-Mo distances we find a greater variation of (2*2.33 Å and 4*2.45 Å) averaging to 2.41 Å. Raman frequencies we expect at 110 cm^{-1}, 135 cm^{-1}, 144 cm^{-1}, 161 cm^{-1}, 187 cm^{-1}, 208 cm^{-1}, 219 cm^{-1}, 252 cm^{-1}, 298 cm^{-1} and 365 cm^{-1}. Co_3Mo_3 has a nearly identical chemical reactivity (μ, η) due to the same calculated electron affinity and ionization potential. Co_5Mo finally resembles almost a regular octahedron.

The Mo atom sits at the top of the octahedron and is 2.37 Å away from the neighboring Co atoms. All the Co-atoms are also nearly equidistant with 2.31 Å and 2.32 Å bond length. We found a $S=\frac{9}{2}$ magnetic ground state

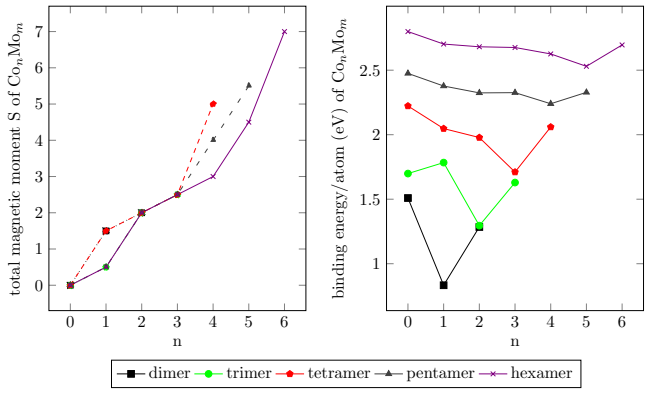

FIG. 5: Various cluster properties with respect to the Mo-concentration: a) total magnetic moment S, b) binding energy (eV/atom)

with an easy plane anisotropy of -0.6 K and a binding energy of 2.57 eV/atom which is the lowest observed for the hexamers. Again the chemical reactivity is closely related Co_4Mo_2 and Co_3Mo_3 due to the nearly identical ionization potential (5.9 eV) and electron affinity (1.4 eV). Additionally, we predict Raman features at 146 cm^{-1}, 158 cm^{-1}, 216 cm^{-1} and 338 cm^{-1}.

IV. GENERAL REMARKS

As already indicated within the discussion of the various-sized clusters there are some general trends that can be observed. As shown in figure 5a) all pure Mo complexes show non magnetic behavior. All pure Co complexes show a magnetic ground state that can be described by

$$S = \begin{cases} \frac{2n+1}{2} & \text{if } n = \text{odd} \\ \frac{2n+2}{2} & \text{if } n = \text{even} \end{cases} \tag{11}$$

where n is the amount of Co in a given cluster[20]. Consequently, the largest magnetic ground state ($S=7$) is observed for the Co_6 cluster. For the mixed clusters we observe an increase in the magnetic moment with increasing Co content, where the magnetic moment is in general due the Co atoms. The magnetic ground state of these clusters can in general also be predicted by equation (11). However in some cases the magnetic moment is quenched, hence a smaller magnetic ground state is found. This seems to be the case for all mixed clusters with a Co content of $n \geq 4$ and also for $n=1$, where we get an $S=\frac{1}{2}$ ground state for $CoMo_2$,$CoMo_4$ and $CoMo_5$ instead the expected $S=\frac{3}{2}$ ground state predicted by the model. Another interesting trend is the steady decrease of the strength of the magnetic anisotropy (regardless of a possible change in the sign of D) with increasing magnetic moment. The only exception are the tetramers where no clear trend is visible.

As shown in figure 5b), there is also a steady increase of the binding energy per atom with increasing cluster size, where the pure Mo clusters are usually a bit more stable than the pure Co clusters for a given total number of atoms x in a cluster. This trend is to be expected as the coordination number increases with increasing cluster size. Starting from pure Mo clusters the binding energy goes down with increasing Co content (see figure 5) . For each cluster size there is a slight decrease in the binding energy with increasing Co content as already discussed in the previous sections, where the mixed cluster with only one Mo atom is always the least stable one.
The change in ionization potential and electron affinity with increasing cluster size can be discussed within the model of conducting spherical droplets as explained elsewhere[55,76–78]. Within this model the cluster is treated as a conducting sphere of radius R and the change of the electron affinity (EA) and the ionization potential (IP) is given by:

$$IP(R) = W + \frac{3}{8}\frac{e^2}{R} \quad (12)$$

$$EA(R) = W - \frac{5}{8}\frac{e^2}{R}, \quad (13)$$

with respect to the charge e and the bulk work function W, which contains the intrinsic information regarding the Fermi level of the bulk material[79]. For very large spheres IP as well as EA should approach this value. This relation can be rewritten in terms of the volume V for a spherical x-atomic cluster[55]:

$$IP(\mathrm{x}) = W + 8.7\mathrm{x}^{-\frac{1}{3}}V^{-\frac{1}{3}} \quad (14)$$

$$EA(\mathrm{x}) = W - 14.5\mathrm{x}^{-\frac{1}{3}}V^{-\frac{1}{3}}. \quad (15)$$

The main conclusion of this model is that one would expect an increase of the electron affinity and a decrease of the ionization potential with increasing cluster size. As shown in table I, this is in general true for the electron affinity and applies also for the ionization potential. It is also very interesting, that for a given cluster size x the ionization potential and the electron affinity increases with increasing Co content. As the chemical potential μ and the molecular hardness η are computed using the ionization potential and the electron affinity (see equation 9 and 10), the trends can also be discussed with respect to the conducting sphere droplet model. Within this model we get:

$$\mu(\mathrm{x}) = -\frac{1}{2}(2W - 5.8\mathrm{x}^{-\frac{1}{3}}V^{-\frac{1}{3}}) \quad (16)$$

$$\eta(\mathrm{x}) = \frac{1}{2}(23.2\mathrm{x}^{-\frac{1}{3}}V^{-\frac{1}{3}}), \quad (17)$$

where a decrease of the chemical potential μ is predicted with increasing cluster size x. This works as a rough estimate to describe the evolution of μ with increasing cluster size x. Another trend is the increase of the chemical potential with increasing Co-content for a given cluster size

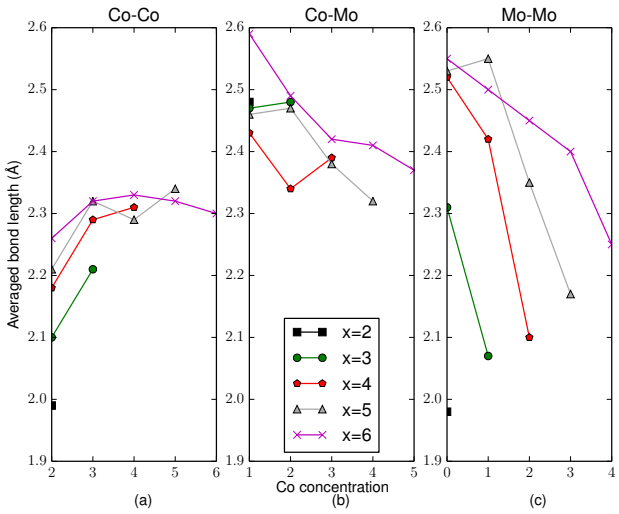

FIG. 6: Average bond distances between neighboring (a) Co atoms, (c) Mo atoms and (b) Co and Mo atoms.

x. This relates directly to the increase in the electron affinity with increasing Co-content as discussed before. Accordingly, the clusters become more stable with increasing Co-content. The molecular hardness η is also predicted to decrease with increasing cluster size x due to the $\mathrm{x}^{-\frac{1}{3}}$ dependency. This works very well for small Co-contents in the clusters and becomes more diffuse for $\mathrm{n} \geq 2$. The reduced molecular hardness for larger clusters results directly in a larger polarizability for these clusters.

Another property is the behavior of the HOMO-LUMO gap. The gap for pure Mo clusters is considerably larger than the gap for pure Co clusters of the same size. Additionally, there is an even-odd effect traceable for all the pure Mo cluster which is also reported in literature[22]. In the pure Co clusters the effect is smaller but nevertheless verifiable. For all clusters of size x ($\mathrm{Co_nMo_m}$ clusters, $\mathrm{x = m+n}$) we observe a steady decrease of the gap with increasing Co content. The exception is $\mathrm{x = 5}$ where again even-odd jumps are visible and $\mathrm{x = 6}$, where the gap of the pure Co hexamer is larger than the one of $\mathrm{Co_5Mo}$. On the other hand we see for $\mathrm{n \geq 2}$ in the $\mathrm{Co_nMo_m}$ cluster an increase in the HOMO-LUMO gap with increasing cluster size.

As discussed in great detail by Baletto et al[80] the average bond length is supposed to shrink with decreasing size of the cluster. This is true for all the discussed clusters and most evident at the evolution of the average Mo-Mo distance for pure Mo clusters (see figure 6c). For a given cluster size x we also observe a decrease in the average Mo-Mo and Co-Mo distance with increasing Co content. The results on the Co-Co distance are not so clear. In figure 6a we see a steady increase in the Co-Co distance for pure Co complexes with the average Co-Co distance of the hexamer slightly lower then the average distance in the pentamer and tetramer, which is in agree-

ment with previous studies[19].

V. CONCLUSIONS

In summary it can be stated that the usual, size-dependent tendencies for metallic clusters are fulfilled. We observe an increase in the binding energy, electron affinity and average bond length with increasing cluster size as well as a decrease in the ionization potential, chemical potential, molecular hardness and the HOMO-LUMO gap. The evolution of the electronic properties (electron affinity, ionization potential) and chemical reactivity (chemical potential, molecular hardness) with increasing cluster size x can be understood within the conducting sphere model. Magnetic properties are mainly governed by the Co atoms in a given Co_nMo_m cluster and magnetic moment rises with increasing cluster size and increasing Co content in a cluster of size x. For nearly all systems we observe a decrease in the magnetic anisotropy (independently of a possible change in the sign of D) with increasing magnetic moment. The only exception is $x = 4$ where no clear trend is visible. This has also been shown experimentally for small Co-clusters[2]. The trends observed for clusters of size x with different chemical compositions can be assigned to the Co content n. For example, the binding energy for $n = 0$ increases with increasing cluster size. This rule applies also for $n = 1,..,6$. Similar conclusion can be made for other properties considered in the present work like electron affinity, chemical potential or bond length. Due to the very interesting magnetic properties these, Co_nMo_m complexes might also be interesting in the field of spintronics, for example for data storage or spin-dependent transport.

Acknowledgments

The authors want to thank the National Science Foundation (XSEDE) for the computational resources, the NordForsk Network on Nanospintronics and the Department of Energy (BES), the Department of Defence (ONR-Global & ITC-ATL) for the financial support of the Summer School "The Como Moments: Theoretical & Computational Modeling of Magnetically Ordered Molecules & Electronic Nano-Transport of Spins: State of Art and Unanswered Questions" within which the idea of this paper was developed. The authors also want to thank the ZIH Dresden and the Cluster of Excellence "Structure Design of Novel High-Performance Materials via Atomic Design and Defect Engineering (ADDE)" which is financially supported by the European Union (European regional development fund) and by the Ministry of Science and Art of Saxony (SMWK) for the computational resources to do the calculations presented in this work.

* TU Bergakademie Freiberg, Institute of Theoretical Physics, Leipziger Strasse 23, D-09596 Freiberg, Germany; simon.liebing@physik.tu-freiberg.de

[1] R. Ferrando, J. Jellinek, and R. Johnston, Chem. Rev. **108**, 845 (2008).
[2] P. Gambardella, S. Rusponi, M. Veronese, S. S. Dhesi, C. Grazioli, A. Dallmeyer, I. Cabria, R. Zeller, P. H. Dederichs, K. Kern, C. Carbone, and H. Brune, Science **300**, 1130 (2003).
[3] D. Fritsch, K. Koepernik, M. Richter, and H. Eschrig, J. Comput. Chem. **29**, 2210 (2008).
[4] T. O. Strandberg, C. M. Canali, and A. H. MacDonald, Phys. Rev. B **77**, 174416 (2008).
[5] R. Xiao, D. Fritsch, M. D. Kuzmin, K. Koepernik, H. Eschrig, M. Richter, K. Vietze, and G. Seifert, Phys. Rev. Lett. **103**, 187201 (2009).
[6] A. Garcia-Fuente, V. M. Garcia-Suarez, J. Ferrer, and A. Vega, Phys. Rev. B **85**, 224433 (2012).
[7] A. Garcia-Fuente, A. Vega, F. Aguilera-Granja, and L. J. Gallego, Phys. Rev. B **79**, 184403 (2009).
[8] B. Kitiyanan, W. Alvarez, J. Harwell, and D. Resasco, Chem. Phys. Lett. **317**, 497 (2000).
[9] B. Hinnemann, P. G. Moses, and J. K. Nørskov, J. Phys. Condens. Matter **20**, 064236 (2008).
[10] J. Kibsgaard, A. Tuxen, K. G. Knudsen, M. Brorson, H. Topsøe, E. Lægsgaard, J. V. Lauritsen, and F. Besenbacher, J. Catal. **272**, 195 (2010).
[11] S. Ganguly, M. Kabir, S. Datta, B. Sanyal, and A. Mookerjee, Phys. Rev. B **78**, 014402 (2008).
[12] M. Pérez, F. Muñoz, J. Mejía-López, and G. Martínez, J. Nanopart. Res. **14**, 1–15 (2012).
[13] M. Castro, C. Jamorski, and D. R. Salahub, Chem. Phys. Lett. **271**, 133–142 (1997).
[14] H.-J. Fan, C.-W. Liu, and M.-S. Liao, Chem. Phys. Lett. **273**, 353 (1997).
[15] C. Jamorski, A. Martinez, M. Castro, and D. R. Salahub, Phys. Rev. B **55**, 10905 (1997).
[16] M. Pereiro, D. Baldomir, M. Iglesias, C. Rosales, and M. Castro, Int. J. Quantum Chem. **81**, 422–430 (2001).
[17] H. Wang, Y. G. Khait a, and M. R. Hoffmann, Mol. Phys. **103**, 263 (2005).
[18] T. O. Strandberg, C. M. Canali, and A. H. MacDonald, Nature Mat. **6**, 648 (2007).
[19] S. Datta, M. Kabir, S. Ganguly, B. Sanyal, T. Saha-Dasgupta, and A. Mookerjee, Phys. Rev. B **76**, 014429 (2007).
[20] A. Sebetci, Chem. Phys. **354**, 196 (2008).
[21] R. Pis Diez, Int. J. Quantum Chem. **76**, 105–112 (2000).
[22] W. Zhang, X. Ran, H. Zhao, and L. Wang, J. Chem. Phys. **121**, 7717 (2004).
[23] F. Aguilera-Granja, A. Vega, and L. J. Gallego, Nanotechnology **19**, 145704 (2008).
[24] M. R. Hoare and J. McInnes, Faraday Discuss. Chem. Soc. **61**, 12 (1976).

[25] N. Arkus, V. N. Manoharan, and M. P. Brenner, Phys. Rev. Lett. **103**, 118303 (2009).
[26] N. Arkus, V. N. Manoharan, and M. P. Brenner, SIAM J. Discrete Math. **25**, 1860 (2011).
[27] R. S. Hoy, J. Harwayne-Gidansky, and C. S. OHern, Phys. Rev. E **85**, 051403 (2012).
[28] A. Tohsaki, H. Horiuchi, P. Schuck, and G. Röpke, Phys. Rev. Lett. **87**, 192501 (2001).
[29] M. D. Hanwell, D. E. Curtis, D. C. Lonie, T. Vandermeersch, E. Zurek, and G. R. Hutchison, J. Cheminf. **4**, 17 (2012).
[30] M. R. Pederson and K. A. Jackson, Phys. Rev. B **41**, 7453–7461 (1990).
[31] K. Jackson and M.R Pederson, Phys. Rev. B **42**, 3276 (1990).
[32] M. R. Pederson and K. A. Jackson, Phys. Rev. B **43**, 7312–7315 (1991).
[33] M.R. Pederson, K.A. Jackson, and W.E. Pickett, Phys. Rev. B **44**, 3891–3899 (1991).
[34] J.P. Perdew, J.A. Chevary, S.H. Vosko, K.A. Jackson, M.R. Pederson, D.J. Singh, and C. Fiolhais, Phys. Rev. B **46**, 6671–6687 (1992).
[35] D. Porezag and M.R. Pederson, Phys. Rev. B **54**, 7830–7836 (1996).
[36] D. Porezag, `Ph.D.thesis`, TU Chemnitz, Fakultät für Naturwissenschaften (1997).
[37] J. Kortus and M. R. Pederson, Phys. Rev. B **62**, 5755 (2000).
[38] M. Pederson, D. Porezag, J. Kortus, and D. Patton, phys. status solidi (b) **217**, 197–218 (2000).
[39] D. Porezag and M. R. Pederson, Phys. Rev. A **60**, 2840–2847 (1999).
[40] J.P. Perdew and Y. Wang, Physical Review B **45**, 13244–13249 (1992).
[41] J.P. Perdew, K. Burke, and Y. Wang, Phys. Rev. B **54**, 16533–16539 (1996).
[42] J.P. Perdew, K. Burke, and M. Ernzerhof, Phys. Rev. Lett. **77**, 3865–3868 (1996).
[43] J. H. van Vleck, Phys. Rev. **52**, 1178 (1937).
[44] M. R. Pederson and S. N. Khanna, Phys. Rev. B **59**, R693–R696 (1999).
[45] M. R. Pederson and S. N. Khanna, Phys. Rev. B **60**, 9566–9572 (1999).
[46] J. Kortus, M. Pederson, T. Baruah, N. Bernstein, and C. Hellberg, Polyhedron **22**, 1871 (2003).
[47] A. Postnikov, J. Kortus, and M. Pederson, Phys. Status Solidi B **243**, 2533–2572 (2006).
[48] C. Van Wüllen, J. Chem. Phys. **130**, 194109 (2009).
[49] R. G. Parr and R. G. Pearson, J. Am. Chem. Soc. **105**, 7512–7516 (1983).
[50] R. G. Parr and W. Yang, J. Am. Chem. Soc. **106**, 4049–4050 (1984).
[51] Jmol, `http://www.jmol.org/` (2015).
[52] M. M. Goodgame and W. A. Goddard, Phys. Rev. Lett. **48**, 135 (1982).
[53] P. Atha and I. Hillier, Mol. Phys. **45**, 285 (1982).
[54] Y. Efremov, A. Samoilova, V. Kozhukhovsky, and L. Gurvich, J. Mol. Spectrosc. **73**, 430 (1978).
[55] M. D. Morse, Chem. Rev. **86**, 1049–1109 (1986).
[56] B. Simard, M.-A. Lebeault-Dorget, A. Marijnissen, and J. J. ter Meulen, J. Chem. Phys. **108**, 9668–9674 (1998).
[57] J. B. Hopkins, P. R. R. Langridge-Smith, M. D. Morse, and R. E. Smalley, J. Chem. Phys. **78**, 1627–1637 (1983).
[58] D. P. DiLella, W. Limm, R. H. Lipson, M. Moskovits, and K. V. Taylor, J. Chem. Phys. **77**, 5263–5266 (1982).
[59] Q.-M. Ma, Z. Xie, J. Wang, Y. Liu, and Y.-C. Li, Phys. Lett. A **358**, 289–296 (2006).
[60] S. Yanagisawa, T. Tsuneda, and K. Hirao, J. Chem. Phys. **112**, 545 (2000).
[61] L. M. Russon, S. A. Heidecke, M. K. Birke, J. Conceicao, M. D. Morse, and P. B. Armentrout, J. Chem. Phys. **100**, 4747 (1994).
[62] D. A. Hales, C. X. Su, L. Lian, and P. B. Armentrout, J. Chem. Phys. **100**, 1049 (1994).
[63] E. K. Parks, T. D. Klots, and S. J. Riley, J. Chem. Phys. **92**, 3813–3826 (1990).
[64] P. Calaminici, F. Janetzko, A. M. Köster, R. Mejia-Olvera, and B. Zuniga-Gutierrez, J. Chem. Phys. **126**, 44108–44110 (2007).
[65] A. Bérces, S. A. Mitchell, and M. Z. Zgierski, J. Phys. Chem. A **102**, 6340 (1998).
[66] V. Koteski, B. Cekić, N. Novaković, and J. Belošević-Čavor, Mat. Sci. Forum **494**, 79 (2005).
[67] R. V. Zee, Y. Hamrick, S. Li, and W. Weltner, Chem. Phys. Lett. **195**, 214 (1992).
[68] S. Yang and M. B. Knickelbein, J. Chem. Phys. **93**, 1533 (1990).
[69] B. Min, C. Wang, and M. Ho, J. Korean Phys.Soc. **39**, 741–745 (2001).
[70] Z.-Q. Li and B.-L. Gu, Phys. Rev. B **47**, 13611 (1993).
[71] A. N. Andriotis and M. Menon, Phys. Rev. B **57**, 10069 (1998).
[72] M. Pereiro, S. Man'kovsky, D. Baldomir, M. Iglesias, P. Mlynarski, M. Valladares, D. Suarez, M. Castro, and J. Arias, Computational Materials Science **22**, 118–122 (2001).
[73] J. L. Rodriguez-Lopez, F. Aguilera-Granja, K. Michaelian, and A. Vega, Phys. Rev. B **67**, 174413 (2003).
[74] J. Guevara, F. Parisi, A. M. Llois, and M. Weissmann, Phys. Rev. B **55**, 13283 (1997).
[75] J. Kortus, T. Baruah, M. Pederson, C. Ashman, and S. Khanna, APL **80**, 4193 (2002).
[76] Smith J. M., AIAA Journal **3**, 648–651 (1965).
[77] D. M. Wood, Phys. Rev. Lett. **46**, 749 (1981).
[78] E. Schumacher, M. Kappes, K. Marti, P. Radi, M. Schaer, and B. Schmidhalter, Berichte der Bunsengesellschaft für physikalische Chemie **88**, 220 (1984).
[79] M. B. Knickelbein, Philos. Mag. B **79**, 1379 (1999).
[80] F. Baletto and R. Ferrando, Rev. Mod. Phys. **77**, 371–423 (2005).